

# A Numerical Investigation on Effects of Asymmetric Angular Position on Performance of Counter Rotating Propeller Systems

Morteza Abasszadeh<sup>1</sup>, Parvin Nikpoor Parizi<sup>2</sup>

<sup>1</sup>Researcher, Urmia University, West Azarbayjan, Iran

<sup>2</sup>Researcher, Sharif University of Technology, Azadi Blvd., Tehran, Iran

(<sup>1</sup>e.m.abbaszadeh@gmail.com, <sup>2</sup>nikpoor.parvin@yahoo.com)

**Abstract-** Due to their unique abilities and high performance counter rotating propeller systems are being implicated to many sensitive applications in propulsion or ventilation proposes. In this study for the first time counter rotating propellers (C.R.P.) have been studied as asymmetric systems by considering the initial angular position of each stage of propeller as the asymmetric parameter. The study carried out on 4, 8 and 12 blade counter rotating propellers to consider effects of increasing blade solidity factor and consequently strength of tip vortex. This study was based on numerical means to acquire results from models. R.S.M. turbulent model was utilized through ANSYS Fluent commercial software package and the method was validated by comparing its results with experimental data of one of references. Final results demonstrated that choosing a proper angular position could improve efficiency of a low performance C.R.P. system by more than 10 percent. In order to investigate distribution of induced values and effects of tip vortices, distribution of Aerodynamic forces also studied along blades.

**Keywords-** Counter Rotating systems; Angular position; Horizontal Element Separation; R.S.M turbulence model.

## I. INTRODUCTION

Counter rotating propellers concept has been studied in recent years as a more energy efficient method in propulsion or air conditioning purposes. As it has been set in Fig. 1 a C.R.P. system consists of two sets of propeller one directly behind the

other one in axial direction spinning in opposite rotational directions. The fundamental premise behind C.R.P. systems is to eliminate tangential velocity which represents energy loss in an axial propeller or fan.

Counter Rotating Propellers (C.R.P.) could produce non-rotating wake which reduces inimical shear stress, vibration, and noise of the system. They also have higher peak efficiency, better off-design performance and a reduced total torque of the system. The increase in peak efficiency and improved off-design performance of counter-rotating systems allow for smaller propulsion or air conditioning units to be installed in different applications.

In early years of introduction of C.R.P. systems, single rotating propeller's analytical methods were used to design and analyze counter rotating propellers. These methods were not accurate enough to gain exact data for vibration and fatigue analysis. Later on, some special methods introduced to design and analysis of counter rotating propellers. First method, developed by Ginzler [1], made no presumption about the distribution of span wise circulation across the blade. It is restricted to the use of aerodynamics that results from propellers, which were built in accordance with the structural constraints existed at the time the theory was developed. This structural restriction was applied in 1943 and is not related to the current state of technology.

Other schemes including SBAC method and a theoretical model developed at United Technologies Research Center (UTRC). SBAC method [2] is very time consuming as it is a design by analysis method and requires data interpolation as well as cross referencing. UTRC method is also time consuming and requires extensive computer memory.

Naiman [3] used a modified strip theory in which approximations for the interference relations from front and aft propeller disks are assumed such that the interference calculations are functions of each propeller disk independently. Naiman used sectional aerodynamic characteristics as a basis for his derivations, so that he could use various families of airfoils and different structural constraints. Sectional circulation to determine the interference relations were also utilized by Naiman. Therefore the method is adaptable to change technology.

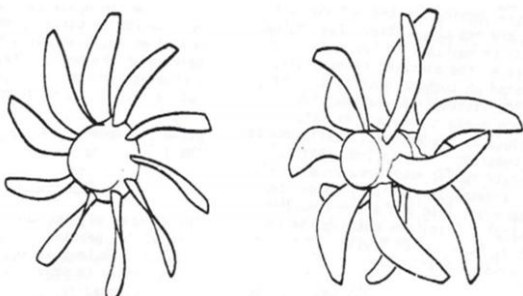


Figure 1. Left: single rotating propeller, Right: counter rotating propeller.



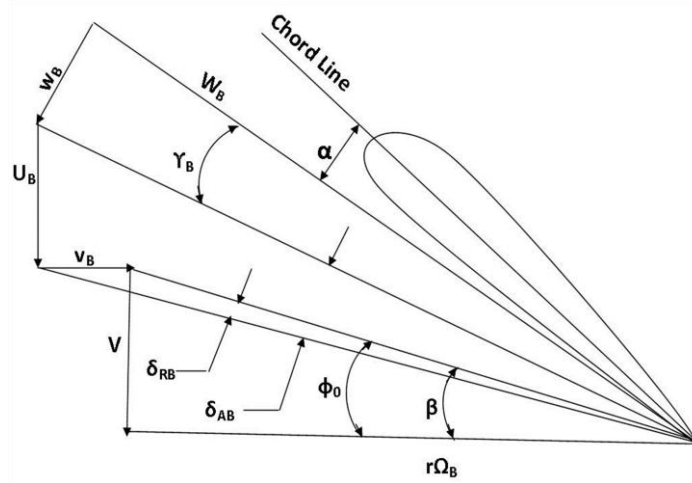


Figure 3. Velocity diagram of rear section [8].

As it described by Korkan, by iterating between the resultant interference velocities and the resultant total velocity, both the interference and total velocities can be found by the following expressions [7]:

$$W_F = r\Omega_F \sec \phi_0 \cos(\phi_F - \phi_0) + u_F \sin \phi_F \quad (1)$$

$$W_B = r\Omega_B \sec \phi_0 \cos(\phi_F - \phi_0) + u_B \sin \phi_B + v_B \cos \phi_0 \quad (2)$$

Where:

$$u_F = X_0 \omega_{1B} \cos \phi_0 \quad (3)$$

$$u_B = X_0 \omega_{1F} \cos \phi_0 \quad (4)$$

$$v_B = 2X_0 \omega_{1F} \sin \phi_0 \quad (5)$$

$$\omega_1 = \phi C_L W / 4X_0 \sin \phi_0 \quad (6)$$

In above equations W is the resultant velocity, u is the axial interference velocity, v is the radial interference velocity,  $\phi_0$  is the element pitch angle,  $\phi$  is the resultant velocity angle,  $\omega$  is the downwash velocity,  $X_0$  is the tip loss factor,  $C_L$  is the lift coefficient, and  $\Omega$  is the rotational velocity.

Davidson [8] has derived Betz's coefficient ( $b_k$ ) using calculus of optimization as:

$$b_k = 4(1 - \eta) \quad (7)$$

Calculation of the reward helical displacement velocity may be accomplished by the expression:

$$w^2 = 2p/\rho[(1 + 0.2M_\infty^2)^{3.5} - 1] \quad (8)$$

Where  $M_\infty$  is infinite stream Mach number, p is the ambient pressure, and  $\rho$  is the density. Using the experimental values of circulation by Theodorsen [6] as a function of  $r/R$  and  $V+w/nD$ , the circulation  $K(x)$  can be found for each radial location as noted in Fig. 4.

Davidson [6] derived a version of Lock's tip-loss factor specific application to counter rotating propellers, which is a well braved function that is different from a single-rotation propeller.

A reformulation for Lock's tip-loss factor that includes drag has been derived and takes the form [5]:

$$X_0 = qs/(2p - qrs) \quad (9)$$

$$p = \frac{\frac{1}{2}}{\cos \phi_0} (\sin \phi_0 + \frac{C_D}{C_L} \cos \phi_0) \quad (10)$$

$$q = \frac{\frac{1}{2}}{2 \sin \phi_0} \quad (11)$$

$$r = \cos^2(\phi_0) - \sin^2(\phi_0) \quad (12)$$

$$s = (\frac{J}{\pi x})/[K(x) \sin \phi_0] \quad (13)$$

Where J is the advance ratio, r is the radial distance, s is the constant of calculation, and q is the freestream dynamic pressure. With the value of  $C_D/C_L$  arrived at through use of the airfoil data banks. Having calculated the solidity-lift coefficient, the differential power coefficients, which are measures of the power absorbed by each propeller disk, can be computed by [5]:

$$\frac{dC_p}{dx} = \frac{\pi^4}{4} (\sec^2(\phi_0) x^4 \sigma C_L (\sin \phi_0 + \frac{C_D}{C_L} \cos \phi_0)) \quad (14)$$

The above equation is integrated to find the total power coefficient ( $C_p$ ) for the power absorbed by both the front and aft propeller disk. The power absorbed is compared to the power input to the propeller by the power plant, which is dictated by the available horse power of the power plant specified in power coefficient form by:

$$C_p = 550 \text{SHP} / \rho n^3 D^5 \quad (15)$$

If the two values of the power coefficient do not match within a given tolerance, Betz's coefficient is adjusted and the power absorbed is recalculated following the outlined procedure.

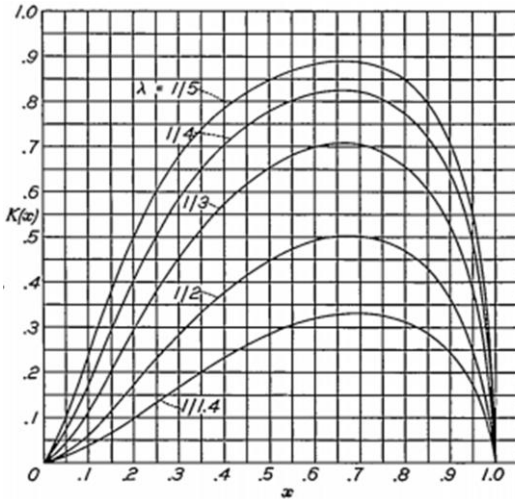


Figure 4. Circular function of dual-rotation propellers [6].

The adjustment made to Betz's coefficient represents alterations in the planform of the propeller blade and thus propeller blade loading. Should the power absorbed be lower or higher than the power input, Betz's coefficient is increased or decreased, respectively. The iteration process is continued until the power absorbed by the propeller is within a predetermined percentage of the power input to the propeller.

The condition of the power absorbed by the propeller being equal to power input, defines the optimum propeller for the given flight conditions since the configuration was designed using the maximum lift-to-drag ratio for the chosen airfoil at each radial location. Also, since the form of Betz's coefficient has been determined through calculus of optimization and used as the iteration parameter, the resulting design is considered to be the optimum counter-rotating propeller for the input condition.

At this point, radial values of the blade planform and twist distribution for each propeller disk can be calculated from:

$$\text{Chord} = 2\pi r \sigma C_L / (\text{No. Blades}) C_L \quad (16)$$

$$\beta = \phi_0 + B + \alpha \quad (17)$$

Where:

$$B_F = \left( \frac{\sigma C_{LF}}{4X_0 \sin \phi_0} \right) (1 + X_0 \cos^2(\phi_0)) \quad (18)$$

$$B_B = \left( \frac{\sigma C_{LB}}{4X_0 \sin \phi_0} \right) (1 + X_0 \cos^2(\phi_0) - 2 \sin^2(\phi_0)) \quad (19)$$

Where  $\sigma$  is the solidity,  $B$  is the interference angle,  $\alpha$  is the angle of attack, and  $\beta$  is the blade twist angle.

The differential thrust and torque are functions of the resultant velocities and calculated by the following expressions:

$$\frac{dT}{dr} = \pi \rho r \sigma C_L W^2 (\cos \phi_0 - \frac{C_D}{C_L} \sin \phi_0) \quad (20)$$

$$\frac{dQ}{dr} = \pi \rho r^2 \sigma C_L W^2 (\sin \phi_0 - \frac{C_D}{C_L} \cos \phi_0) \quad (21)$$

Integration of above equations results in value of thrust ( $T$ ) and torque ( $Q$ ), hence the thrust coefficient ( $C_T$ ), torque coefficient ( $C_Q$ ) and efficiency ( $\eta$ ), comes from:

$$C_T = \frac{T}{\rho n^2 D^4} \quad (22)$$

$$C_Q = \frac{Q}{\rho n^2 D^5} \quad (23)$$

$$C_P = 2\pi C_Q \quad (24)$$

$$\eta = C_T J / C_P \quad (25)$$

### III. C.F.D. METHOD

As it is experienced and verified in many previous investigations, since R.S.M. turbulence model accounts for the effects of streamline curvature, swirl, rotation, and rapid changes in strain rate in a more rigorous manner than one-equation and two-equation models, it has greater potential to give accurate predictions for complex flows. So in this investigation R.S.M. model was chosen to analyze designed model. As Smith [9] described in his work the ensemble-averaged, steady, incompressible Navies-stokes equations in Cartesian tensor notation can be stated as:

Continuity Equation:

$$\frac{\partial}{\partial x_i} (\rho u_i) = 0 \quad (26)$$

Momentum Equation:

$$\frac{\partial(\rho u_i u_j)}{\partial x_i} = -\frac{\partial \rho}{\partial x_i} + \frac{\partial}{\partial x_j} (\bar{\tau}_{ij} + \tau_{ij}) \quad (27)$$

The mean viscous stress tensor  $\bar{\tau}_{ij}$  is approximated as:

$$\bar{\tau}_{ij} = \mu \left( \frac{\partial u_i}{\partial x_j} + \frac{\partial u_j}{\partial x_i} \right) \quad (28)$$

The time-averaged Reynolds stress tensor,  $\tau_{ij} = -\rho \overline{u_i' u_j'}$ , in the above equation is not known and, thus, models are needed to express it in terms of the solution variables.

For an R.S.M., the Reynolds-averaged transport equations are solved for the Reynolds stress tensor,  $\tau_{ij}$ , the modeled equations for which are:

$$\frac{\partial \tau_{ij}}{\partial t} + \frac{\partial (u_k \tau_{ij})}{\partial x_k} = -G_{ij} - \Phi_{ij} + D_{ij} + \varepsilon_{ij} \quad (29)$$

Where:

$$G_{ij} = \rho P_{ij} = -\left( \rho \overline{u_i' u_k'} \frac{\partial u_j}{\partial x_k} + \rho \overline{u_j' u_k'} \frac{\partial u_i}{\partial x_k} \right) \quad (30)$$

$$\Phi_{ij} = -C_1 \frac{\rho \varepsilon}{k} \left( \overline{u_i' u_j'} - \frac{2}{3} k \delta_{ij} \right) - C_2 \left( G_{ij} - \frac{2}{3} G \delta_{ij} \right) \quad (31)$$

$$D_{ij} = \frac{\partial}{\partial x_k} \left( \left( \frac{\mu_e}{\sigma_t} \right) \frac{\partial \overline{u_i' u_j'}}{\partial x_k} \right) \quad (32)$$

$$\varepsilon_{ij} = \frac{2}{3} \rho \varepsilon \delta_{ij} \quad (33)$$

In which  $C_1 = 2.5$ , and  $C_2 = 0.55$  are model constants.

In (29), from left to right, we have the time rate of change of the Reynolds stress at a fixed point, the net convection of Reynolds stress by the mean flow to the fixed point, local production ( $G_{ij}$ ) of Reynolds stress, local pressure strain ( $\Phi_{ij}$ ), net diffusive transport ( $D_{ij}$ ) of Reynolds stress to a fixed point, and local dissipation tensor. Equation (28) provides an expression for each of the six Reynolds stresses. These six simultaneous equations for stress are to be solved along with the equations of turbulence kinetic energy dissipation rate.

The R.S.M. method was utilized through ANSYS Fluent commercial software package which have been proved as a reliable asset in several previous investigations. In this study in order to validate use of the method, "Master airscrew F/G 11\*4" sample from [8] was modeled and results of numerical tests was compared to experimental DATA. As it is demonstrated in Fig. 5 numerical results was fairly close to experimental results.

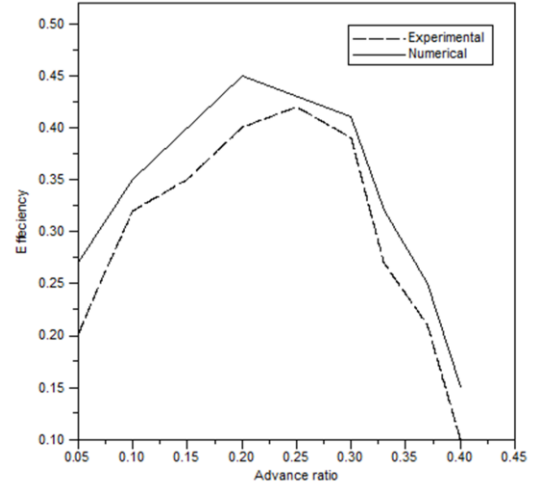


Figure 5. validation of the numerical method.

#### IV. CONCEPTS AND METHODS

In 1943 Theodorsen stated [17] that efficiency of a single rotating propeller would be maximized if its wake shapes as flat rotational disks behind the propeller. In years this has been learnt that Theodorsen's statement was an optimistic phrase. In fact wake of a propeller is look like rotating sheets, in number of the blades, behind the rotor. Downstream of the rotor also would not be effected invariantly [16]; the regions which are covered by rotating sheets would have more axial and rotational velocity [Fig. 6].

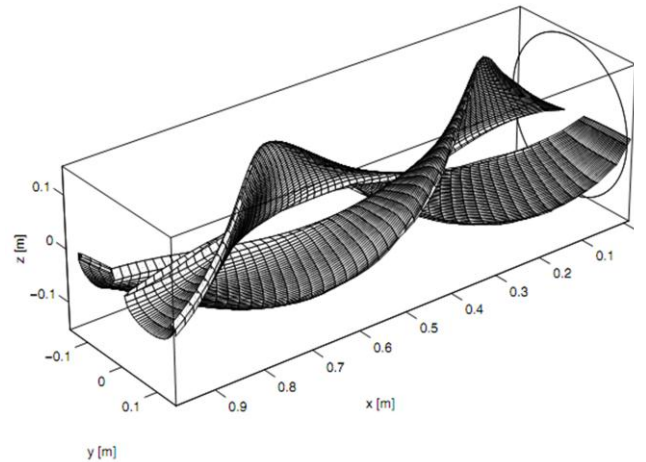


Figure 6. rotating sheets beyond rotating disk [16].

In which  $\psi$  is angular position,  $\tau$  is axial position from the disk and  $H$  is the pitch step of the rotating disk and can be determined by:

$$H = \frac{V + \omega r}{2\pi n} \quad (34)$$

The rational conclusion would be that the initial angular position of the rear disk (considering the first disk angular position is in 0 degrees), could be determined by (34). But in this investigation a series of models was designed and tested by different initial angular positions to investigate the reliability of that conclusion.

In terms of model design main interest was to eliminate any specifications that limit results to any geometrical or environmental conditions. In this study a simple non-twisted blade with cross section of NACA2412 was utilized to all 3 models.

Non-twisted blades are being utilized in propeller which by their nature requires low twists such as electrical fans, small size propulsion fans a vertical lift generating systems to reduce costs of production [16].

Design of a non-twisted blade is same as design of a twisted blade but instead of repeating the calculations for each horizontal element specification of a referential element (recommended by lock to be the element in 0.7 of disk radius), would be generalized in to all the elements. In this study, specifications of the referential element calculated by the Korkan method. The propeller disk had a radius of 50 cm and chord of the blade was 5 cm. rotational speed of the models was set to 30 R.P.S. operating in a 5 m/s extreme velocity.

In any propeller design procedure whether it is single rotating or after designing initial geometry there is an iteration loop to optimize the geometry by changing each elements chord or pitch angel. Considering the models that Theodorson utilized to present his famous theory about mass

coefficient [17]. A differential analysis about C.R.P. systems is not corresponding to performance of the models; therefore the iteration loop was omitted in this study.

## V. RESULTS

Design of a non-twisted blade is same as design of a twisted blade but instead of repeating the calculations for each horizontal element specification of a referential element (recommended by lock to be the element in 0.7 of disk radius), would be generalized in to all the elements. In this study, specifications of the referential element calculated by the Korkan method. The propeller disk had a radius of 50 cm and chord of the blade was 5 cm. rotational speed of the models was set to 30 R.P.S. operating in a 5 m/s extreme velocity.

In any propeller design procedure whether it is single rotating or after designing initial geometry there is an iteration loop to optimize the geometry by changing each elements chord or pitch angel. Considering the models that Theodorson utilized to present his famous theory about mass coefficient [17]. A differential analysis about C.R.P. systems is not corresponding to performance of the models; therefore the iteration loop was omitted in this study.

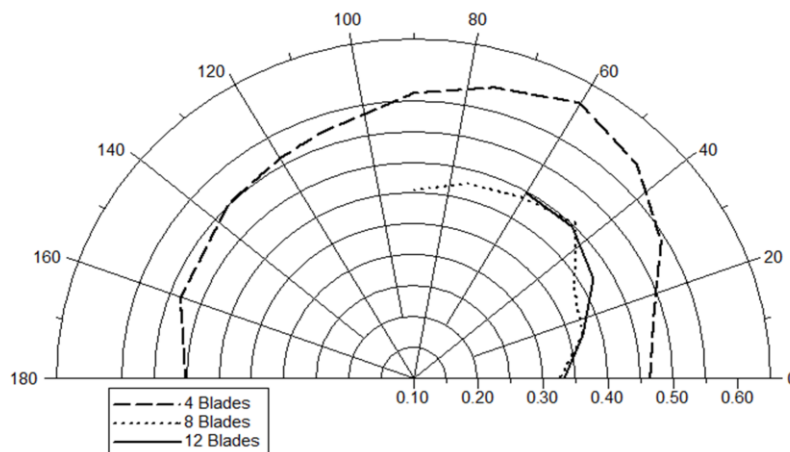


Figure 7. Overall efficiency variation in different angular Position.

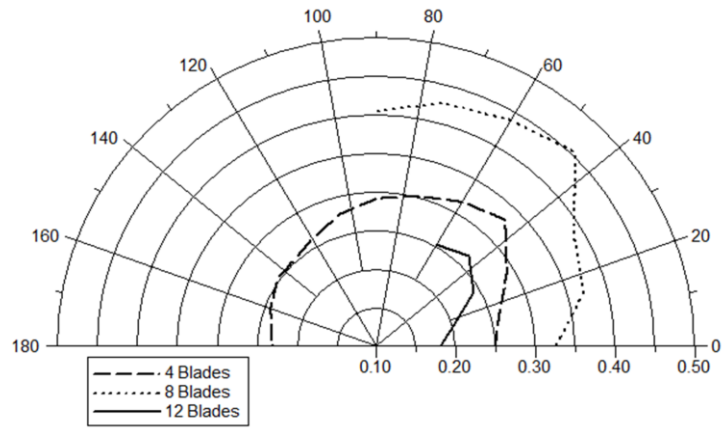


Figure 8. Front blade efficiency variation in different angular Position.

Results indicate that an asymmetric angular position configuration also would have considerable effects on front disk performance. Fig. 8 shows that efficiency of front disk would be maximized in an angular position less/more than the position that total efficiency maximizes. This effect is probably due to effects of performance of rear disk on induced angles of front section. Such effects can be seen in (2) to (6).

One of the less experienced ways to analyze an axial propeller or fan is to study the aerodynamic distribution profiles. Slight drops in the end of distribution profiles can demonstrate strength of tip vortices.

Experiences of the authors proved that use of Horizontal Element Separation method can illustrate distribution profiles with an acceptable accuracy [10].

Distribution of aerodynamic forces which has been illustrated in Fig. 9 and Fig. 10 shows there are not any significant changes in behavior of thrust distribution profiles. This fact suggests that distribution of induced angles (which are highly function of tip vortex effects) remains same as symmetric C.R.P. systems.

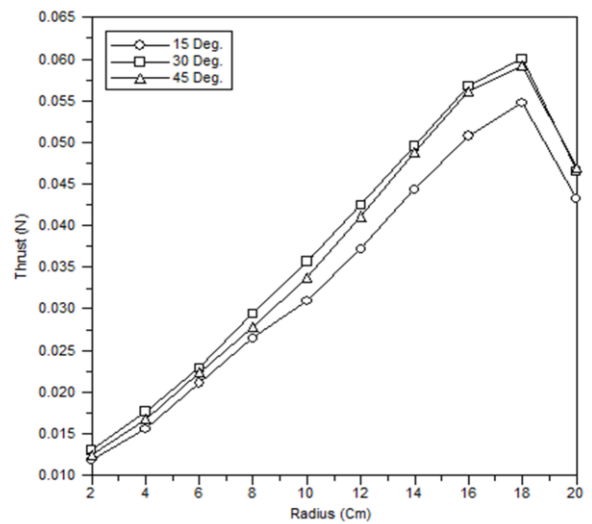


Figure 10. Thrust distributions in different asymmetric angular positions, 12 blades model, rear blade.

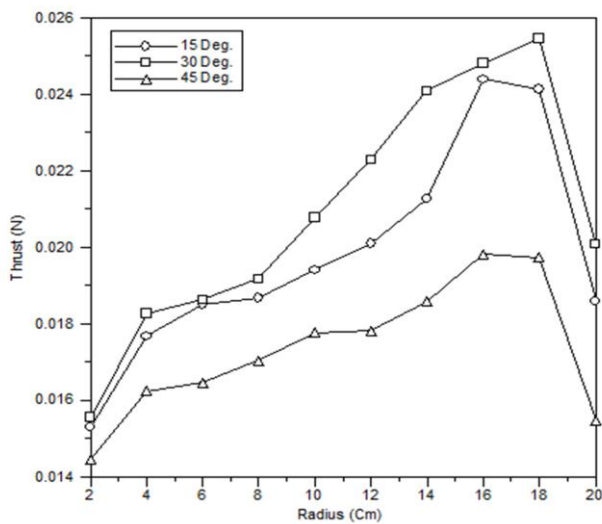


Figure 9. Thrust distributions in different asymmetric angular positions, 12 Blade model, Front blade.

## VI. CONCLUSION

Results of this study proved that a proper angular position and a precisely designed C.R.P. system can have nearly 10 percent advantage to a conventional symmetric C.R.P. system. But main achievement of this investigation was not about precise measures in optimum positions or performance enhancements. The precise measures and actual behavior of asymmetric C.R.P. system must be studied in more extensive investigations. Main achievement of this study was proving the fact that there are parameters beside geometrical specifications that must notified in any further attempt to optimize or design of C.R.P. systems.

## REFERENCES

- [1] Ginzel, F. "Calculation of Counter Rotating Propellers," NASA TM 1208, March 1949.
- [2] "Advanced Prop-Fan Engine Technology (APET) Definition Study," NASA 3-23045, 1982.

- [3] Naiman, I. "Method of Calculating Performance of Dual Rotating Propellers from Airfoil Characteristics," NACA ARR 3E24 (WR.L-330), May 1943.
- [4] T. Teodorson, "The Theory of Propellers Determination of the Circulation Function and the Mass Coefficient for Dual Rotating Propellers," NACA report No. 775, 1939.
- [5] Pyle, S.C., "A Numerical Method for the Design and Analysis of Counter-Rotating Propellers," M. Sci. thesis, Texas A&M university, June 1984.
- [6] Davidson, E.R. "Optimization and Performance Calculation of Dual Rotating Propellers," NASA TP 1948, Dec. 1981.
- [7] S. C. Playlc, K. D. Korkan, E. VonLavante, "A Numerical Method for the Design and Analysis of Counter-Rotating Propellers," *AIAA J. Propulsion*, Vol.2, No.1, Jan-Feb 1986.
- [8] Brandt J.B, Selig M.S, "Propeller Performance Data at Low Reynolds Numbers," 49<sup>th</sup> AIAA Aerospace Sciences Meeting, Orlando, 2011.
- [9] Benini E, "Significance of Blade Element Theory in Performance Prediction of Marine Propellers," *Journal of Ocean Engineering*, Vol.3 No.1, pp. 957-974, 2004.
- [10] P. Pratumnopharat, P.S. Leung "Validation of Various Windmill Brake State Models Used by Blade Element Momentum Calculation," *Journal of Renewable Energy*, Vol.3 No.6, pp.3222-3227, 2011.
- [11] Tenguria N, Mittal N.D., Ahmed S, "Investigation of Blade Performance of Horizontal Axis Wind Turbine Based on Blade Element Momentum Theory (BEMT) Using NACA Airfoils," *International journal of science engineering and technology*, Vol. 2, No. 12, 2010, pp. 25-35, 2010.
- [12] Chakravarty U.K, "Section Builder: An Innovative Finite Element Tool for Analysis and Design of Composite Rotor Blade Cross-Sections," *Journal of Composite Structures*, Vol. 9, No.2, pp.284-294, 2010.
- [13] M.J. Smith, M.J. Patil, D.H. Hodges, "CFD-Based Analysis of Non-Linear Aeroelastic Behavior of High Aspect Ratio Wings," AIAA 2001-1582.
- [14] M. Abbaszadeh, P. Nikpour, M. Shahrooz, "Analysis of Distribution of Thrust, Torque and Efficiency of a Constant Chord, Constant Pitch C. R. P. Fan by H. E. S. Method," *World Academy of Science, Engineering and Technology*, July 2011.
- [15] M. Abbaszadeh, M. Shahrooz, B. Farhaniyeh, "Effects of Using Different Arrangements of Fanlets on Performance of Twisted Axial Aerial Fans", *Proceedings of ASME Turbo Expo*, Copenhagen, Denmark, 2012.
- [16] Wagner, S. "Flow Phenomena on Rotary Wing Systems and Their Modeling," Plenary lecture at the 76th Annual GAMM Conference, Bremen, April 6-9, 1998.
- [17] T. Teodorson, The theory of propellers determination of the circulation function and the mass coefficient for dual rotating propellers, 1939, N.A.C.A report No. 775.